Total Removal of Unwanted Echoes in Harmonic Phase MRI (TRUE-HARP)

K. Z. Abd-Elmoniem[1] and J. L. Prince[1,2]

[1]Electrical and Computer Engineering, Johns Hopkins University, Baltimore, Maryland, United States, [2]Department of Radiology, Johns Hopkins University Medical School, Baltimore, Maryland, United States

Introduction: Harmonic phase imaging (HARP)[1] employs spatial cosine tagging of the longitudinal magnetization at the end-diastole. The first harmonic peak is filtered later on at each cardiac phase to extract both in-plane displacement and strain. Interference from the DC and the conjugate peaks is detrimental to HARP processing. A remedy for that is to use a small filter size which reduces interference but with the penalty of reducing the resolution and the dynamic range. Ringing artifact is also common filtering artifact. CANSEL[2] was advised to eliminate the T_1-relaxation echo and the complex conjugate echo using ten different displacement-encoded acquisitions. A modification to CANSEL was later proposed that reduces the total number to only five breath-hold acquisitions. Both methods are quite long and sensitive to slice change and drift between scans and thus suffered from mis-registration. In this work, we present a single breath-hold imaging scheme that totally remove the interference artifact permitting higher resolution strain mapping without the need for preprocessing registration. Preliminary human results show significant reduction of the interference artifacts in the calculated strain maps.

Table1: Slice-selective tagging parameters for TRUE-HARP

	θ_1	θ_2	Gx	Gy
I_{A1}	90^o_x	90^o	G	0
I_{B1}	90^o_x	-90^o	G	0
I_{C1}	90^o_y	90^o	G	0
I_{A2}	90^o_x	90^o	0	G
I_{C2}	90^o_y	90^o	0	G

Theory: Consider a cosine-modulated SPAMM image has an intensity $I_{A_1}(x,y)$ where

$$I_{A_1}(x,y) \propto \rho(x,y)e^{j\varphi_E(x,y)}(1+\cos(\varphi_x)) = \rho(x,y)e^{j\varphi_E(x,y)}\left[1+\left(e^{j\varphi_x}+e^{-j\varphi_x}\right)/2\right]$$

φ_x is the displacement-encoded phase contrast, resulting from tagging (this case is in x-direction), and $\varphi_E(x,y)$ is the phase from inhomogeneity. In addition to I_{A_1}, the following sets are acquired

$$I_{B_1}(x,y) \propto \rho(x,y)e^{j\varphi_E(x,y)}(1-\cos(\varphi_x)) \quad I_{A_2}(x,y) \propto \rho(x,y)e^{j\varphi_E(x,y)}(1+\cos(\varphi_y))$$
$$I_{C_1}(x,y) \propto \rho(x,y)e^{j\varphi_E(x,y)}(1+\sin(\varphi_x)) \quad \text{, and} \quad I_{C2}(x,y) \propto \rho(x,y)e^{j\varphi_E(x,y)}(1+\sin(\varphi_y))$$

From these sets, and with the following complex manipulation,

$$\rho e^{j(\varphi_E \pm \varphi_x)} = \left[I_{A_1} - I_{B_1} \pm j\left[2I_{C_1} - \left(I_{A_1}+I_{B_1}\right)\right]\right]/2,$$
$$\rho e^{j(\varphi_E \pm \varphi_y)} = \left[\left[2I_{A_2} - \left(I_{A_1}+I_{B_1}\right)\right] \pm j\left[2I_{C_2} - \left(I_{A_1}+I_{B_1}\right)\right]\right]/2$$

x-, and y-displacement-encoded phases are extracted as follow

$$\varphi_x = \left[\angle\rho e^{j(\varphi_E+\varphi_x)} - \angle\rho e^{j(\varphi_E-\varphi_x)}\right]/2, \qquad \varphi_y = \left[\angle\rho e^{j(\varphi_E+\varphi_y)} - \angle\rho e^{j(\varphi_E-\varphi_y)}\right]/2$$

φ_x and φ_y are identical to HARP phases with the advantage of not being cropped and therefore, have high resolution and dynamic ranges.

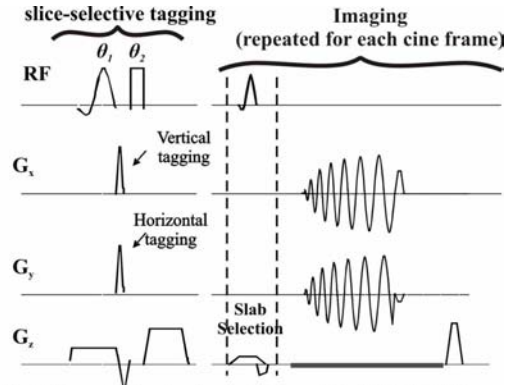

Fig.1 Slice-selective tagging building unit for TRUE-HARP

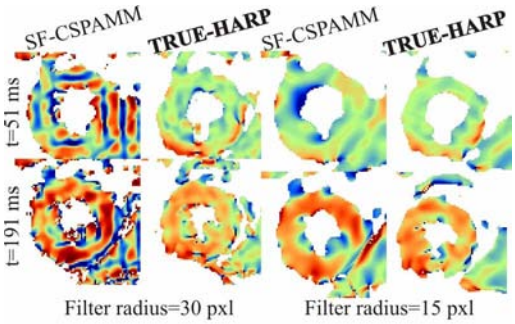

Fig.2 Err maps from SF-CSPAMM and TRUE-HARP

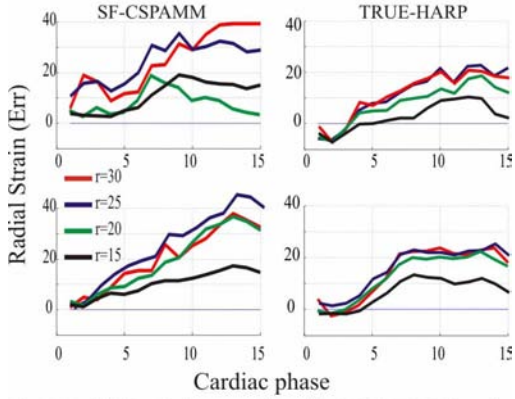

Fig.3 Radial Strain time-profile with SF-CSPAMM and TRUE-HARP with different HARP filter size

Methods: ***Imaging:*** TRUE-HARP pulse sequence was implemented on a commercial Philips 3T-Achieva whole body system. The pulse sequence consists of five short slice-selective tagging sequences to acquire I_{A1}, I_{B1}, I_{C1}, I_{A2}, and I_{C2} images (see Fig.1). The acquisitions differ in the values of θ_1, θ_2, G_x, and G_y as shown in Table.1. Image processing was performed off-line on a personal computer. One healthy 33-years old male volunteer and five pigs were scanned using VECG triggered spiral imaging with a 15 ms acq. window, 4 spiral readouts, 144 samples/spiral, FOV =300mm, slice thick.=8mm, TR=25 ms, and tag spacing=8 mm. The total scan was completed in a single breath-hold in 20 heart beats. For comparison, Slice-following images were collected with a 9 ms acq. window, 12 spiral readouts, 192 samples/spiral, and tag spacing=12 with vertical and horizontal tagging were applied in separate breath-holds.

Analysis: Strain map was computed from both TRUE-HARP and SF-CSPAMM datasets using HARP analysis with different filter sizes (radii: 15, 20, 25, and 30 pixels) with Fourier resolution of 10, 7.5, 6, and 5 mm, respectively.

Results As shown in Fig.2, the larger the HARP filter is, the more interference in the strain map. Since myocardial radial stretching corresponds in k-space to the harmonic peaks coming closer, interference artifacts get worse. That results in artifactual and unreliable radial strain maps. Artifacts were substantially reduced with TRUE-HARP even with larger filter. Err time-profile at two points is plotted in Fig.3. Notice the chaotic behavior with larger HARP filter applied to CSPAMM data while TRUE-HARP results tend to agree.

Conclusion: A single breath-hold tagging pulse sequence was proposed to reduce the artifacts in myocardial strain maps when applying HARP analysis. In-vivo results show a significant reduction of artifacts even with large filter size suggesting the possibility of getting high-resolution and more reliable strain maps.

References: 1.)Osman:TMI'00, 2.)Epstein:MRM'04